Single Crystals of Chain-Folded Copolyterephthalamides

Sabine Manet, Carmen Tibirna, Julie Boivin, Christine Delabroye, and Josée Brisson*

Département de chimie, Centre de recherche en sciences et ingénierie des macromolécules, Faculté des sciences et de génie, Université Laval, Québec, Québec, Canada G1K 7P4

Received October 18, 2005; Revised Manuscript Received November 30, 2005

ABSTRACT: Crystallization of copolyaramides composed of rigid poly(*p*-phenylene terephthalamide) segments (containing 3−11 aromatic cycles) and short amine aliphatic chains (5−10 CH_2 groups) was studied. Crystallization was induced at room temperature by slow saturation with methanol vapors of sulfuric acid solutions. In electron diffraction, the 3AR6DA, which has monodisperse rigid blocks, exhibits weak but typical single crystal diffraction, with relatively sharp diffraction spots. Other wARnDAs, for which the rigid blocks are polydisperse, show a similar diffraction diagram albeit with lower resolution and considerable peak broadening, indicating that considerable disruption of the crystal phase has taken place. All observed diagrams correspond to the *hk*0 level, and chains are perpendicular to the lamellar plane. Atomic force microscopy observations show that most crystals are multilamellar, the thickness of each lamella increasing regularly with the number of aromatic groups in the rigid segment. The average lamellar thickness value is in agreement with the expected rigid segment length. It is therefore concluded that the addition of a short aliphatic chain fragment allows chain folding to occur.

Introduction

Folding is a prominent feature in proteins, where it is mainly controlled by the amino acid sequence and governs the observed three-dimensional structure essential to protein activity. In silk proteins, rigid homopolymer units are connected via more flexible sequences, thus achieving a spectacular control on liquid crystallinity, crystallite form, and size,[1] which in turn provides extraordinary properties to silk. Bioengineering of sequences is an established path to controlling folding and structure of amino acids,[2] while the field of "foldamers" aims at developing synthetic oligomers or polymers which fold to predetermined structures in solution.[3]

Chain folding of synthetic polymers in the solid state was first reported for polyethylene crystals[4] and firmly established by the work of Fischer,[5] Keller,[6] and Till.[7] Although polymer crystallization has been intensively studied, many interrogations remain, and the introduction of new experimental techniques, such as atomic force spectroscopy, as well as studies on controlled model compounds, such as folding linear or cyclic oligomers, has resulted in a renewed interest in kinetic and morphological studies of polymer crystallization, as attested by various reviews.[8−10] Nevertheless, in the vast majority of studies reported in the literature, crystallization is controlled mainly via external conditions, such as temperature, stress, and pressure. Crystallization control via sequence design has received comparatively little attention. This is unfortunate, as chain folding control could allow fine-tuning of the crystalline morphology of the polymers, for example by fixing the crystal thickness through selection of an appropriate polymer sequence, by modulating the surface properties of crystals by the adjunction of functionalized folds, by favoring growth in specific dimensions by selecting folding groups that from folds preferentially in a given crystallographic direction, or by favoring the existence of tie chains that pass through two adjacent lamellae as compared to chain reentry.

Chain-fold-inducing strategies have been proposed in the literature for synthetic polymers, whether in the context of crystallization or in solution. These include intrachain or interchain interactions,[3,11] steric hindrance-inducing groups,[12,13] and rigid units with tailored distances and angles.[14]

In the present work, it was chosen to induce crystallization through variation of the flexibility of the polymer sequence: A rigid (or more exactly semirigid) para-linked aramide block was selected as the crystallizable unit, whereas a short, flexible aliphatic segment was used as the fold inducer, resulting in polymers with the following structure:

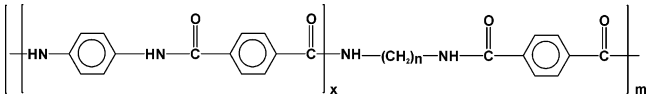

These are abbreviated *w*AR*n*DA, in which $w = 2x + 1$, where *w* is the average number of successive aromatic moieties per rigid block, *n* the number of CH_2 groups per flexible block, and *m* the number of macrorepeat units per chain. The value of *w* was varied from 3 to 11 to allow investigation of the effect of rigid block size on crystallization. The value of *n* was varied from 5 to 10, which allowed to study the influence of the length of this segment on the regularity of the crystals obtained.

This approach is similar, but inverse, to that used by Schmidt, Decher, and Mésini, which also modulated flexibility to induced chain folding. In their case, however, the rigid spacer formed the fold, the more flexible segment being allowed to crystallize. These polymers are also related to, but differ from, foldamers, as the *w*AR*n*DA incorporate relatively long homopolymer sequences and are not designed to fold in solution, and rod−coil copolymers, as the flexible sequence or *w*AR*n*DA is too short to form self-assembled phase-separated morphologies,[15] such as for some aramide−aliphatic block copolymers which have been reported presently.[16] Therefore, the *w*AR*n*DA belong to a separate class of copolymers, which could be describes as hinged copolymers, the flexible spacer acting as a built-in molecular hinge.

The chemical structure of the rigid blocks used here is similar to that of poly(*p*-phenylene terephthalamide) or PPTA. The use of para-linked aramides as the rigid block provides various advantages: Synthesis is well established, the para-linked

* To whom correspondence should be addressed.

10.1021/ma052248k CCC: $33.50
Published on Web 01/07/2006

Table 1. Characterization of Polymers Used in This Study

block copolymer	macromonomer I_p	copolymer M_v (g/mol)	copolymer M_w[a] (g/mol)	copolymer M_n[a] (g/mol)	copolymer I_p[a]	copolymer DP_v[b]	copolymer DP_{sec}[c]
7AR5DA	1.2	6500	8600	1800	4.7	6.9	2.1
7AR6DA	1.2	6500	5700	2000	2.8	7.5	2.3
7AR7DA	1.2	7900	7500	2400	3.2	8.1	2.6
7AR8DA	1.2	10 200	8600	2400	3.5	10.4	2.6
7AR9DA	1.2	7900	7900	2200	3.5	4.3	2.4
7AR10DA	1.2	9100	8000	2600	3.1	9	2.8
3AR6DA	1.00	5500	7900	4000	2.0	11.4	9.0
6AR6DA	1.2	2800	3600	2000	1.8	3.3	2.6
7AR6DA	1.2	6500	5700	2000	2.8	7.5	2.3
8AR6DA	1.1	3300	5200	2300	3.1	3.1	2.3
9AR6DA	1.3	3700	5000	1700	2.9	3.1	1.6
11AR6DA	1.6	2000	3400	1600	2.1	1.3	1.2

[a] As estimated from SEC of allylated derivatives. [b] As calculated using M_v, the average mass of a block M_b and the mass of a flexible block M_f, $DP_v = M_v/(M_b + M_f)$. [c] As calculated using M_n, the average mass of a block M_b, and the mass of a flexible block M_f, $DP_{sec} = M_n/(M_b + M_f)$.

homopolymers are known to exhibit liquid crystallinity even when interspersed to some degree with aliphatic segments,[17] and only two polymorphs,[18,19] differing mostly by the type of chain packing, are known. Crystal structure models have been proposed for both forms,[18,20,21] although for form I, experimental evidence points to the need to reevaluate the space group and, consequently, chain packing.[22] Single crystals with the *c* axis perpendicular to the thin section of the crystals of form I have been obtained using an evaporation polymerization technique[22] and will be useful to compare with the results obtained in the present study. Other attempts at growing single crystals resulted in ribbonlike crystals which did not show any chain folding (*c* axis not perpendicular to the thin section of the crystals),[23,24] which was proposed to be due to the high rigidity of the backbone. Further, this polymer is known not to exhibit a long period.[25] This could be related to its rigidity, which hinders regular chain fold formation. The main drawback in studying aramides such as PPTA or the *w*AR*n*DA copolymers is the impossibility of studying them in the melt, as they decompose before melting above 400 °C. The present article will therefore focus on crystallization from solution of these copolymers and on the resulting morphologies.

Experimental Section

Copolymer synthesis and characterization have been described elsewhere.[26] Molecular weights, polydispersities I_p, and degrees of polymerization DP (expressed as the average number of macrorepeat units, each composed of one rigid block and one flexible segment per copolymer chain) are reported in Table 1. The poly(hexamethylene terephthalamide) homopolymer, which is abbreviated 1AR6DA here, was obtained by interfacial polymerization following the work of Shashoua and Eareckson[27] and was only used for X-ray diffraction comparison. Pure PPTA diffraction diagrams were taken from averaging of the fiber diffraction diagrams of Kevlar 49 (DuPont) fibers, which are composed of the pure PPTA homopolymer.

Crystallizations were performed on 0.1% w/v concentrated sulfuric acid solutions. The solutions were introduced in a 10 mm diameter test tube. A second test tube of similar size was filled with methanol. Both test tubes were place in a desiccator, and methanol vapors slowly condensed in the sulfuric acid solution. Crystals were isolated by centrifugation, and the solvent changed to pure methanol until the pH of the solution was equal to that of pure methanol.

Crystalline suspensions was allowed to dry on a glass slide and introduced in 1 mm diameter glass capillaries. Wide-angle X-ray diffraction spectra (WAXD) were taken using the GADDS software on a Bruker diffractometer consisting of a Kristalloflex 760 generator, a three-circle goniometer, and a Hi-Star area detector. The generator produced a graphite monochromatized copper radiation (Cu Kα = 0.154 18 nm) under operating conditions of 40 kV and 40 mA.

A Digital Instrument Nanoscope Multimode SPM AFM microscope consisting of a model 5137 JVH scanner coupled with the Nanoscope IIA controller, and software was used for atomic force microscopy. The scan size was of 2 μm, and the scan rate 1 Hz was used. Methanol crystal suspensions were deposited on a silicon wafer (Montco Silicon Technologies, Inc.) previously washed, successively, with a sulfochromic acid solution, deionized water, and methanol. Samples were then dried for 2 days in a vacuum oven at 60 °C prior to use. Images were recorded in the tapping mode and height of sections measured using the Nanoscope 5.12r5 software.

Crystal suspensions were deposited on carbon-coated 100 mesh copper electron microscope grids. Some electron micrographs and diffraction patterns of the crystals were recorded on a JEOL EM1200FX electron microscope functioning at 80 kV under low dose conditions. A tungsten filament was used, and the minimal camera length of 15 mm selected for diffraction, which was recorded using Kodak SO-163 films. Most samples were studied on a JEOL 1230 microscope functioning at either 80 or 100 kV, again under low-dose conditions. On this microscope, a LaB_6 filament was used, and a Gatan CCD camera was used to record the diffraction patterns. In some cases, 1.5 nm gold shadowing was deposited on the grids prior to their observation, using a homemade evaporator equipped with a CVC diffusion pump going down to 5×10^{-6} Torr and an Inficon XTM/2 thickness monitor.

Results

Crystallization. In the present work, various crystallization methods were used, including the addition of a nonsolvent at high temperature and vapor saturation in a desiccator of a polymer solution. All crystallized samples were first observed under optical microscope to verify the presence of birefringent nonaggregated material, and the most promising samples were observed in an electron microscope.

Sulfuric acid, dimethylpropyleneurea, and *N*-methylpyrrolidone were used as solvents, whereas precipitating agents included distilled water, various alcohols (methanol, ethanol, 1-propanol, 2-butanol, 1,4-butanediol, 2-methylpropanol, phenol), ethylene glycol, and acetone (not used with sulfuric acid solutions, as these react together). All analyses reported here were performed on the best crystals, which were obtained by the vapor saturation method from sulfuric acid solutions, while using methanol as the precipitant.

As sulfuric acid could cause degradation of the polymers, crystallizations were performed at room temperature. Crystallization time was relatively long, and temperature fluctuations were liable to occur. This may explain the appearance, in some of the samples, of smaller and larger crystals present in the same vials.

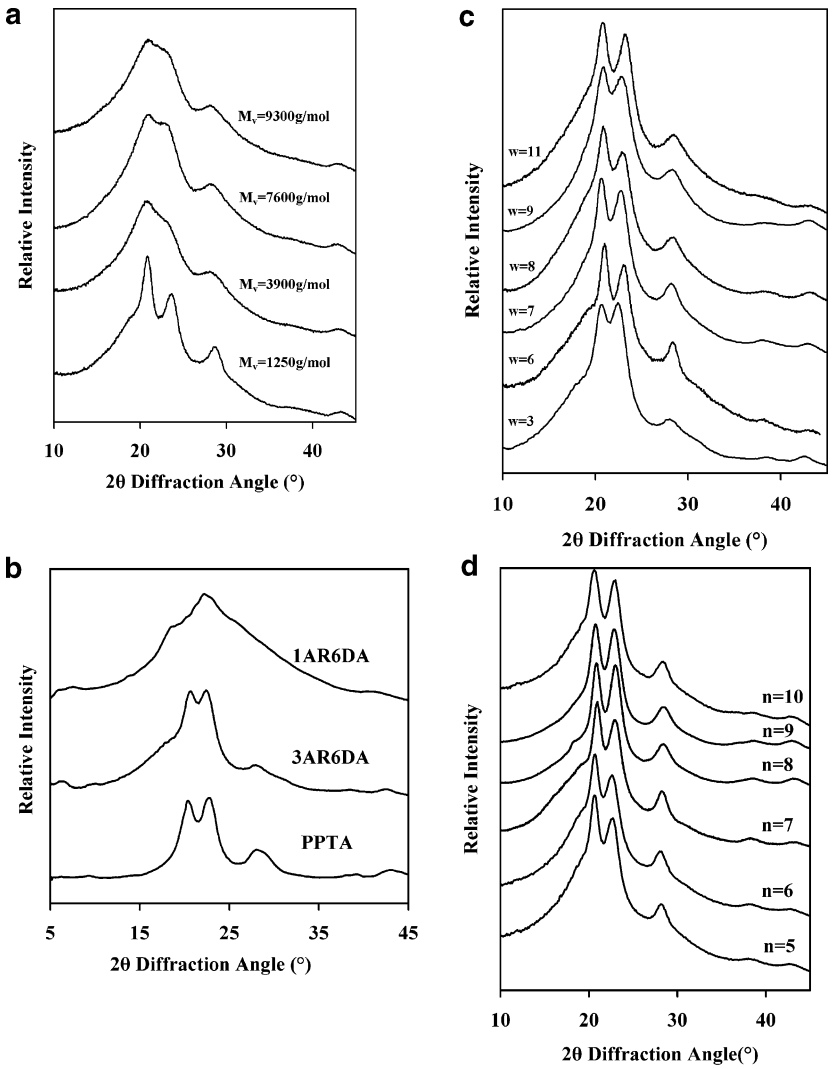

Figure 1. X-ray diffraction diagrams of rigid−flexible copolymers (a) 6AR*n*DA of various molecular weights. (b) Comparison between 3AR6DA and two homopolymers, 1AR6DA or nylon-6T and pure PPTA. (c) Flexible segments composed of six methylene units, with variable rigid block length *w* (*w*AR6DA). (d) Seven benzamide groups per rigid block on average, with variable number of CH_2 unit *n* per flexible segment (7AR*n*DA).

X-ray Diffraction Characterization of Crystalline Suspension. Copolymer crystals were characterized by X-ray diffraction, as reported in Figure 1. As can be seen in Figure 1a, peak width increases with molecular weight of the polymer, indicating that shorter chains crystallize in a more highly organized fashion and have higher crystallinity. In Figure 1b, the 3AR6DA aliphatic−aromatic copolymer is compared to pure PPTA and to the poly(hexamethyleneterephthalamide) homopolymer (1AR6DA), often called nylon-6T. The PPTA reported is in its form I, with major diffraction peaks at 2θ angles of 20.7° (0.4 nm) and 22.8° (0.39 nm), and a medium-intensity peak around 29° (0.3 nm), whereas in form II the peak positions are slightly different, with a medium-intensity peak at 17.4° (0.51 nm), the strongest peak at 22.8° (0.39 nm), and a medium-intensity peak at 27.9° (0.32 nm).[19,28] As expected, in our case, form I, first reported by Northolt, is observed for 3AR6DA, whereas a different crystalline phase is observed for 1AR6DA,[29] with diffraction peaks around 18.6° (0.48 nm), 22.2° (0.40 nm), and 25.8° (0.35 nm).

Changes of crystallinity with flexible chain length can be observed in Figure 1c for the copolymers having $n = 6$. All copolymers have similar peak positions and relative intensities, indicating that the major crystalline form is also form I, as expected. These mainly differ by the relative crystallinity, as can be seen from the height of the amorphous halo appearing as a broad shoulder near 20°. The same can be seen when varying the flexible segment length, *n*, as reported in Figure 1d.

Quantification of the crystallinity has been performed using the FFCRYST program written by Vonk[30] on the basis of the method proposed by Ruland.[31] No completely amorphous samples being available, a subtraction of diffraction spectra with different crystallinities was performed to yield a suitable amorphous phase spectrum. Resulting crystallinity values are reported in Figure 2. When varying the number of CH_2 groups per aliphatic segment, *n*, for the same number of aromatic cycles per rigid unit, $w = 7$, crystallinity appears to be maximal for $n = 8$ to 9 CH_2 groups, although the differences are not large considering other variables affecting crystallinity, such as molecular weight and temperature and condition fluctuations during sample preparations. On the other hand, when comparing the crystallinity of polymers with different rigid unit sizes, *w*, no variation, within experimental error, could be found with the exception of the 3AR6DA copolymer.

Electron Microscopy. Transmission electron microscopy images of typical crystals obtained by solution crystallization appear in Figure 3. These are generally thin oval lathes such as those in Figure 3a, often multilayered and showing a tendency

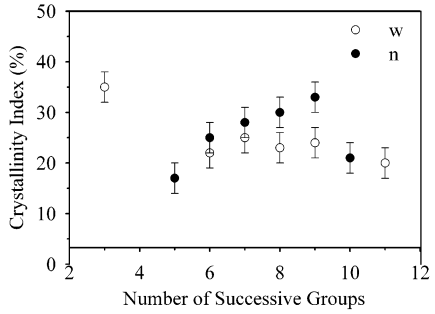

Figure 2. Crystallinity changes for two series of copolymers. Closed symbols: polymers with average block size *w* of 7 aromatic cycles, but with different aliphatic segment length *n*. Open symbols: polymers with aliphatic segment of 6 CH_2 units, but with varying rigid segment length *w*.

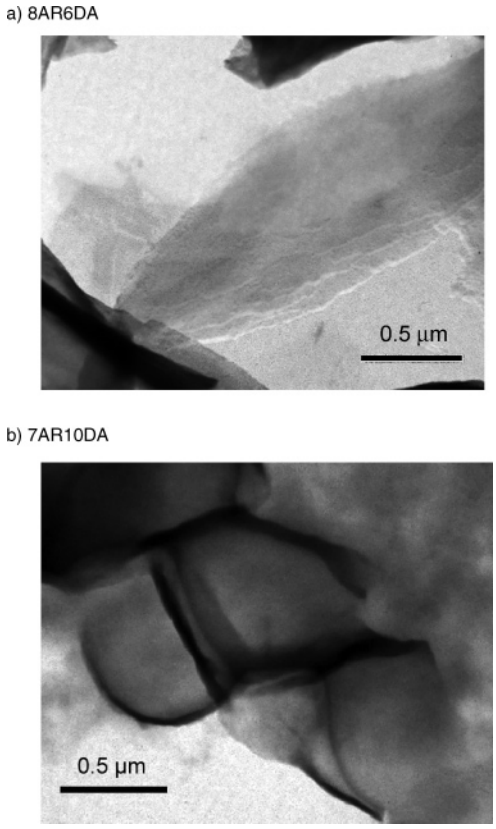

Figure 3. Electron microscopy photographs of shadowed copolymer single crystals (a) 8AR6DA and (b) 7AR10DA.

to fold onto themselves when deposited on the carbon-coated copper grids. Lateral dimensions are approximately of 0.5 × 2.0 μm and vary within a given sample and from one sample to another. The crystal surface is not entirely uniform, and overgrowths or decorations appear as well as multilayering. The general oval shape is adopted by most *w*AR*n*DA crystals studied, with the exception of 7AR9DA and 7AR10DA, in which the crystals show two different forms: a fine needlelike form, too small to allow single crystal diffraction, and much large lathes, seen in Figure 3b, more rectangular than oval in shape, which also show very little surface decoration, if any, contrary to the oval crystals. The crystal edges also appear to "curl over" easily, as can be seen in Figure 3b.

The crystals do not degrade as rapidly as most polymers under the electron beam, which is attributed to the high thermal stability of the PPTA-like rigid blocks, and yield diffraction patterns typical of single crystals, as can be seen in Figure 4

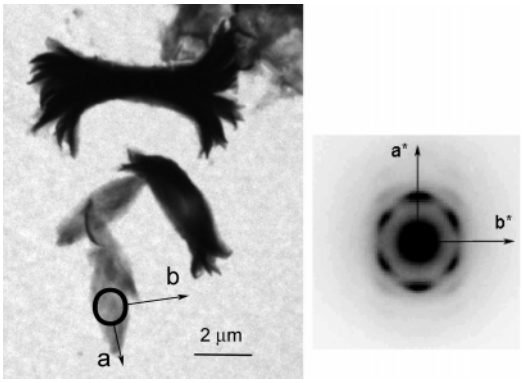

Figure 4. Unshadowed electron diffraction image and diffraction of 8AR6DA.

for a typical 8AR6DA crystal (unshadowed) and its corresponding diffraction pattern. The *a*-axis of the unit cell is parallel to the long direction of the lathes, and the *c*-axis is perpendicular to the plane of the crystals, as expected for folded chain crystals. In this picture are shown two types of crystals: the usual oval lathes, described above, as well as lamellar stacks or sheaves appearing as if standing on edge. These stacks are very thick, as expected from the lateral size of the crystals, the electron beam is almost completely absorbed, and no diffraction study can be performed on these.

Figure 5 shows typical electron diffraction diagrams of the various *w*AR*n*DA crystals. All are very similar in terms of position and symmetry of the most intense diffraction spots, including the 7AR10DA. All *w*AR6DA electron diffraction diagrams are reported, as these show variations in resolution and peak width. In the 7AR*n*DA series, however, only $n = 5$ and 10 are shown, as all 7AR*n*DA are similar, variations between individual crystals of a given sample being comparable to those between different samples. For 3AR6DA, for which the rigid block was the smallest of the series, crystal thickness was also the smallest, diffracted intensity was low, and therefore signal-to-noise ratio not very good. A good resolution and peak sharpness were nevertheless observed, clearly indicating that these were crystalline; the crystalline order is comparable, although slightly lower (less diffraction spots being observed) to that previously reported for the polymerization evaporation method.[22] In many cases, single crystals were aggregated, which resulted in arcing of the diffraction diagrams. For the other copolymers of the series, diffraction spots are considerably more spread out in all direction. For these, the best resolution is observed for 9AR6DA.

Finally, in many cases, although a major population of oval lathes exists, smaller needlelike precipitates can also be seen. These are too small to allow recording of an electron diffraction pattern under low dose, and therefore their crystalline polymorph cannot be ascertained. Considering the strong overlap of the most intense diffraction spots in powder X-ray diffraction diagrams, for the known PPTA crystal forms, the presence of a small portion of crystals having a different crystalline form cannot be excluded.

AFM Observations. AFM was used to further study the morphology of the samples. Typical AFM tapping mode images of *w*AR*n*DA crystals appear in Figure 6. These show substantial decorations atthe lamella surface, and in many cases, the multilayer nature of the crystals can clearly be distinguished. Shapes resemble those observed by electron diffraction, namely oval lathes, with the exception of 7AR9DA and 7AR10DA, where the crystals tend to be more rectangular in shape, and

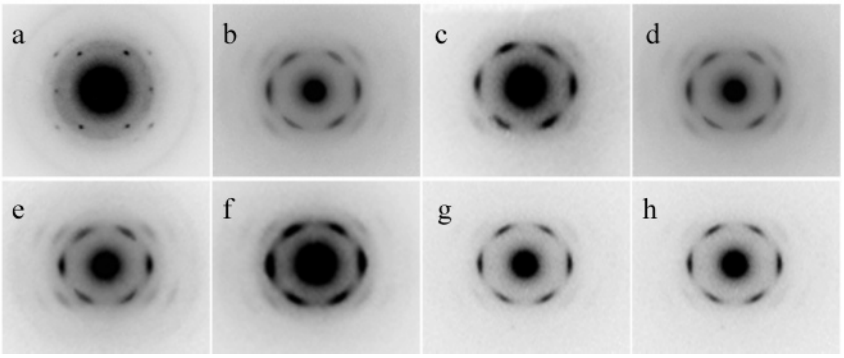

Figure 5. Electron diffraction diagrams for *w*AR*n*DA copolymers: (a) 3AR6DA, (b) 6AR6DA, (c) 7AR6DA, (d) 8AR6DA, (e) 9AR6DA, (f) 11AR6DA, (g) 7AR5DA, and (h) 7AR10DA.

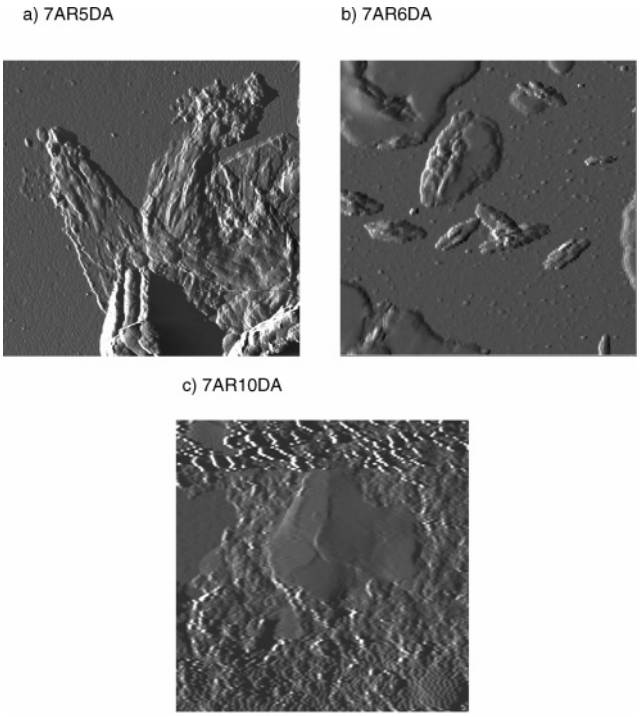

Figure 6. AFM micrographs (phase contrast mode) of representative crystals (2 μm width): (a) 7AR5DA, (b) 7AR6DA, and (c) 7AR10DA.

the surface appears smoother, as already noted in the electron microscopy study.

Very narrow and thick structures with a finer subdivision could also be seen on some of the pictures, as if crystals were standing on-edge, again as was the case in electron microscopy images (Figure 4).

Discussion

Copolymer Characterization. The ideal copolymer to use for crystallization design would be perfectly regular, long enough to chain fold while short enough so that crystallization be favored. Experimental limitations, however, resulted in polymers which, with the exception of 3AR6DA, did not fit these ideal requirements. Two different synthesis approaches were used. In the first, a series of protection/deprotection ensured that block length was monodisperse.[32,33] Because of the number of synthetic steps required, block lengths were limited to $w = 3-9$, and molecular weights were lower than those expected for folding to occur (from one to two rigid blocks per polymer chain), which was attributed to purification problems of the macromonomers. In a second approach, described in more detail in a previous article,[26] synthesis of block lengths up to $w = 13$ was possible in a two-step technique, by the use of an excess of one of the two reagents (phenylenediamine) during the first, rigid macromonomer synthesis step.[26] However, this yielded polydisperse rigid blocks, with the exception of $w = 3$, for which the macromonomer was pure phenylenediamine, terephthalic acid end-capped at both ends. These polydisperse block copolymers were used in the present study, as in terms of number of rigid blocks per polymer chain, they fitted the requirements of the crystallization design, although the polydispersity of the blocks reduced regularity. Crystallization is however bound to be affected by this polydispersity of the rigid blocks. Reported polydispersities of the macromonomers, I_p, were determined using a combination of NMR-determined number-average molecular weights and viscosity-average molecular weights.[26]

In the resulting *w*AR*n*DA copolymers, *w* indicates an average number of aromatic groups and not the exact number. The value of *n*, the number of CH_2 groups in the aliphatic amine, is however an exact value. Molecular weight and polydispersities of the resulting copolymers were estimated via size exclusion chromatography of allylated derivatives, following the work of Russo and co-workers.[34] Degrees of polymerization (DP) reported in Table 1 refer to the number of macrorepeat units (composed of one rigid block and one flexible block each and expressed as "*m*" in the polymer chemical formula, as reported in the Introduction) per chain.

It is noteworthy that the polymers studied here have similar M_w, M_n, and I_p, and therefore similar DPs and "macrorepeat units", although the exact number differs when using the number-average values obtained by size exclusion chromatography (SEC) or the viscosity averages. Two main exceptions occur. First, 3AR6DA has a molecular weight considerably higher and polydispersity lower, which is attributed to the higher purity and monodispersity of the macromonomomer. Second, 11AR6DA has a lower molecular weight and an average number of rigid blocks of only 1.2 per polymeric chain. Results using this polymer should therefore be viewed with caution, as chain length is not sufficient to ensure that chain folding has taken place. In all other cases, around 2−3 rigid segments are present per polymeric chain as calculated using SEC measurements.

Requirements for Crystallization: Regularity and Size of Regular Sequence. A universal requirement for crystallization is polymer chain regularity. However, even an atactic polymer can crystallize partially if sufficient chain segments have a regular conformation, as shown by the observation of small crystallinity degrees in some atactic polymers, such as PVC or PE. It has recently been shown by Le Fevere et al.[12] that the presence of "defects" regularly placed along PE chains does

not hinder crystallization if the regular segments are long enough and if the defects are placed in a strictly periodical manner.

With the exception of 3AR6DA, shorter block lengths have a tendency to yielding less perfect crystals (as attested by electron diffraction), at least for the polydispersities used here. It must be stressed that the shorter block lengths were also the least polydisperse, as determined by a combination of NMR spectroscopy and viscosimetry measurements. Therefore, polydispersity is not the sole factor affecting crystalline order: Longer rigid, crystallizable block length favors crystalline order despite a higher polydispersity. This is at variance with results on PE blocks by le Fevere de ten Hove, Penelle, Ivanov, and Jonas, where strict monodispersity was found essential for crystallization.[12] In the present study, short rigid segments crystallized as well as, or almost, as longer rigid segments, in contrast again with the case of PE, where defective crystals were formed when the regular crystallizable sequences were too short (22 CH_2 units). These two effects are tentatively attributed to the rigidity of the crystallizing unit and/or to the formation of hydrogen bonds in the polyaramides studied here, which could increase crystallization tolerance to length or dispersity of the crystallizable units.

The 3AR6DA is clearly behaving at variance with other *w*AR*n*DA: It is considerably more crystalline, as seen by X-ray powder diffraction in Figure 2, and although average crystal size is low, crystal perfection is much higher, as seen from the electron diffraction pattern reported in Figure 5a. It is also the only copolymer studied here which has a completely monodisperse rigid block. This clearly shows the influence block length polydispersity: When it is higher, crystallinity is always lower and crystalline order poorer, as reflected by diffraction spot width, no matter what the block size or the flexible unit is.

No minimum molecular weight is required for a molecule to crystallize, and indeed higher molecular weights are often detrimental to polymer crystallization. However, oligomers may adopt crystalline structures different, in terms of conformation and packing, from that of the parent polymers. It was therefore of interest to determine what was the minimal length of the rigid terephthalamide-based polymers for crystallization to proceed in the same crystal form as that of PPTA. As shown by the X-ray diffraction diagrams in Figure 1, a succession of three aromatic amide sequences, or $1^1/_2$ repeat unit, is sufficient for the crystal phase of PPTA to appear. Electron diffraction of the *w*AR*n*DA, depicted in Figures 4 and 5, yields patterns which are very similar in peak position, relative intensities, and systematic absences to those obtained previously.[22] Further, the relative intensities and peak positions also match those of the Northold PPTA form I. This confirms that the copolymers crystallize in the same crystal structure as the homopolymer. The 2AR6DA was however not available for comparison, and it was therefore not possible to confirm if a length corresponding to a single unit cell is sufficient for crystallization to occur in the PPTA crystalline form, as proposed recently by Chen et al.[35]

Observed Morphology of Crystals. Only three reports of monocrystals of PPTA have been published in the literature. Jackson and Chanzy[23] and Takahashi et al.[24] have obtained ribbonlike crystals in which the repeat units grew along the long direction of the ribbons and not perpendicular to the crystal surface, which indicates that these were not chain-folded crystals but probably fibrils. Liu et al.[22] obtained crystals directly from melt polymerization crystallization, in which molecular weight may be low enough for the crystals to contain the complete chain and therefore in which chain folding may not be present. In no case were single crystals obtained by the more usual solvent recrystallization techniques, which may be related the relative rigidity of the chain. This made the choice of PPTA for the rigid block particularly interesting, as electron diffraction diagrams could easily be identified, while obtaining chain-folded crystals from solution has been impossible until now.

Two main observations can be made on crystal morphology, as seen in Figure 3: First, they do not present regular edges, their appearance being that of mostly oval or spindlelike sheaves. Second they present, for the most part, surface decorations and multiple layers. These could be related to the fact that the crystals were grown in nonequilibrium conditions and that coagulant concentration varied throughout crystallization. This can undoubtedly explain the observed crystal size dispersion within a sample. However, crystal form and presence or absence of lamellar decorations both varied with flexible chain length, as can be observed in Figures 3 and 6, although all samples were crystallized under the exact same conditions. We therefore propose that, although the use of nonequilibrium conditions must have contributed to the crystal morphology, it cannot explain alone the present observations.

The appearance of rounded crystal edges is not exceptional. Similar sheaves or lenticular crystals have been reported previously for solution-grown crystals[36] as well as solid-state crystallizations[37,38] and polycaprolactone surface crystallization.[39] These are frequently observed at higher temperatures and can be explained using the Sadler rough-surface theory of crystal growth[9,40] and the Frank crystal growth model.[41] In the present case, although the crystals were obtained at room temperature, it is proposed that factors similar to those involved in high-temperature roughening could account for the observed crystal shapes. Crenellations of the type proposed by Sadler would certainly be compatible with the polydispersity of the crystallizing blocks. It is difficult to determine with certainty whether the polydispersity of the crystallizing blocks, the inappropriate fold length, the nonequilibrium growth conditions, or a combination of these factors is responsible for the appearance of the rounded edges. It is noteworthy that, for longer flexible chain length (7AR9DA and 7AR10DA, as seen for example in Figure 6c), crystal surface appears smoother, as if a longer chain length could, at least in part, compensate for polydispersity by facilitating crenellations. This could explain the observed increase in crystallinity up to $n = 9$, as observed in Figure 2, whereas the decrease observed for $n = 10$ could be due to a greater difficulty to crystallize when the flexible chain reaches a certain value, although further work will be necessary to verify these points.

Likewise, the observed surface decorations are not unique. They can be a sign of crystal degeneration due to the rigidity of the blocks, as observed for PEEK and other rigid polymers, which yielded ill-formed lamellae with jagged edges, knobbly internal structure, and small sizes.[42] It is difficult, due to the mode of crystal growth used here, to distinguish crystal degeneration due to rigidity from other factors favoring surface decorations, such as nonequilibrium growth conditions or crystallization temperature, as increasing this parameter would be liable to produce chain scission and therefore lower molecular weights, resulting in oligomers crystallizing without the need of chain folding. The fact that similar crystal morphologies were observed for *w*AR6DA when $w = 5-11$, while electron diffraction showed that crystalline order was different in these crystals, indicates that the surface decorations are likely not due to crystal degeneration.

Surface decorations can also be due to the presence of screw dislocations, giving rise to splaying of the crystals. Although the observed decorations to not resemble the classical edge dislocation images, they may be imperfect or aborted dislocations, as some splayed lamellar stacks have been observed standing on-edge in both electron and atomic force microscopy. Whether the aggregation is based solely on interactions (van der Waals or electrostatic) or screw dislocations or whether a few flexible chains are incorporated along the *c*-axis of the crystals and actually pass through two or more aggregated crystallite layers is difficult to ascertain.

Effect of Flexible Chain Length. The introduction of flexible segments in a rigid chain is nothing new, as attested by the growing body of literature on rod−coil polymers. When the flexible segment in large, it phase-separates, yielding a variety of fascinating self-assembled structures. If very small, the chains could neither segregate in isolated domains nor chain fold. These would then either interfere with crystallization, thus decreasing crystallinity, or be incorporated in the crystalline domains as defects, thus lowering crystalline order. We therefore targeted a selection of a chain sizes approximately in the range expected for chain folds. Selection of the flexible chain length was dictated mainly by molecular modeling simulations, which show that, for nylon-6, a five-carbon aliphatic chain was sufficient for adjacent reentry.[43] For other polymers, 7−8 bond folds have been proposed.[44] Studies on short oligomers which chain-fold during crystallization have also corroborated that regular folding occurs for around 7−8 bond sections.[9] Further, it has been proposed that the number of bonds per fold depends on geometrical conditions dictated by the space group and by the difference in chain height in the adopted space group.[45] Therefore, flexible chain lengths were varied from 5 to 10 CH_2 groups to allow for the differences in space groups and unit cell dimensions of PPTA. The same rigid macromonomer blocks were used to synthesize 7AR5DA to 7AR10DA, and therefore the blocks have the exact same molecular weights and polydispersities.

As was observed in Figure 5, crystalline order is comparable in individual crystals obtained for various chain lengths, although total crystallinity of samples was found to vary slightly, as observed by X-ray diffraction in Figure 2. These observations are in agreement with the absence of incorporation of the flexible segments in the crystal lattice but do not prove that no incorporation has taken place or that folding it occurring.

Morphologies differ with chain length, however, as can be seen in Figure 3. Whereas shorter chains, for 7AR5DA to 7AR8DA, have approximately the same spindle-shaped crystals, for the longer blocks, mixtures of small needlelike crystalline precipitates and larger, uniform crystals with a form close to a rectangular shape occur. These are of much more regular surface and have little or no decorations, and the multilamellar nature is less marked. Electron diffraction on these crystals shows the same resolution, crystalline form, and order as those of the spindlelike crystals.

Modulation of the crystalline morphology may therefore partially be obtained by an appropriate design of the flexible segment. It has long been shown by infrared spectroscopy that adjacent chain reentry leads to sharp folds.[46,47] Short folding segments could therefore be involved in adjacent retry. However, in the present case, shorter chains ($n = 5-7$) do not lead to uniform surfaces of the type one would expect for adjacent reentry, but lead to lamellar stacking. This could be due to the occurrence of block polydispersity, which should induce protruding rigid blocks at the fiber surface, favoring step formation on the crystal surface, as the shorter aliphatic chains are not able to compensate by reentering at the original crystal surface. Longer flexible segments may be able to do this, and in this case the defects would not lead to lamellar steps at the crystal surface, but to a larger inhomogeneous amorphous layer, composed of aliphatic loops, end chains but also a certain number of rigid blocks. Further work will therefore be necessary to elucidate the effect of the flexible chain length on crystallization of monodisperse rigid−flexible copolymers, by choosing a rigid unit for which it is possible to better control polydispersity.

Height of the Crystal Lamella as Compared to Rigid Block Size. Comparison of observed electron diffraction patterns with the previously published electron diffraction unit cell parameters of PPTA phase I clearly indicates that the "*c*"-axis lies perpendicular to the oval lathes. This is compatible with chain folding. However, chain folds are not necessarily present, as the size of the chain is not incompatible with the thickness of lamellar stacks obtained. Two types of information are therefore necessary to ascertain that chain folding has taken place: comparison of crystalline order with respect to the length of the flexible segment and determination of individual lamella thickness. It has already been observed that electron diffraction of 7AR*n*DA is comparable for $n = 5-10$. Therefore, increase in chain length does not increase disorder, which indicates that flexible chains are not incorporated in the crystalline phase as defects and must therefore be segregated at the crystal surface, presumably in the form of chain folds. However, a more direct evidence that chain fold does occur is the size of the individual lamella or lamellar decorations, which should be approximately equal to the size of the crystallizable blocks if flexible segments do form folds.

Thicknesses were observed via transverse sections of the AFM images, as appears in Figure 7 for two representative examples. Sections show that crystals grow in well-defined steps or lamella, and transversal cuts allow estimation of the thickness of each lamella. In Figure 7a, the inserted image shows an AFM height image, as well as the section on which the height was measured. The scan starts at the left of the image, and the height is close to zero until the 0.3 μm position in length is reached, where the AFM tip meets the crystal. Height then steps to ∼15 nm, which corresponds to approximately two rigid blocks of size 5.6 nm each, as calculated by the crystal phase *c*-axis value and weight-average molecular weight of the rigid blocks. At ∼0.4 μm in length, the tip rises again, on a crystal decoration this time, as seen in the inserted image. A height of 28 nm is reached, and the tip stays around this height for 0.1−0.2 μm and then falls back on the original bilamellar surface at around 0.55 μm position in length. The tip then steps briefly, around 0.65 μm in length, on a 6 nm high lamellar surface, corresponding to a unilamellar surface, and then goes down on the substrate. In the 8AR*n*DA, and indeed in most *w*AR*n*DA, it was impossible to find a section where a single lamella was present, secondary lamella or surface decorations invariably being observed.

For the 7AR10DA, as seen in Figure 7b, the crystal surface is clearly lower, as multilamellar crystals are scarce. As seen on the image insert, the scan begins at the left, on a surface where smaller, needlelike crystals are present, and therefore height fluctuates around 1−3 nm. Around 0.27 μm position in length, the tip raises suddenly to 7 nm in height, and then returns to 6 nm, a value close to the calculated value of 5.1 nm using the weight-average molecular weight of the rigid block and the value of the *c*-axis for the crystal unit cell. In this case, therefore,

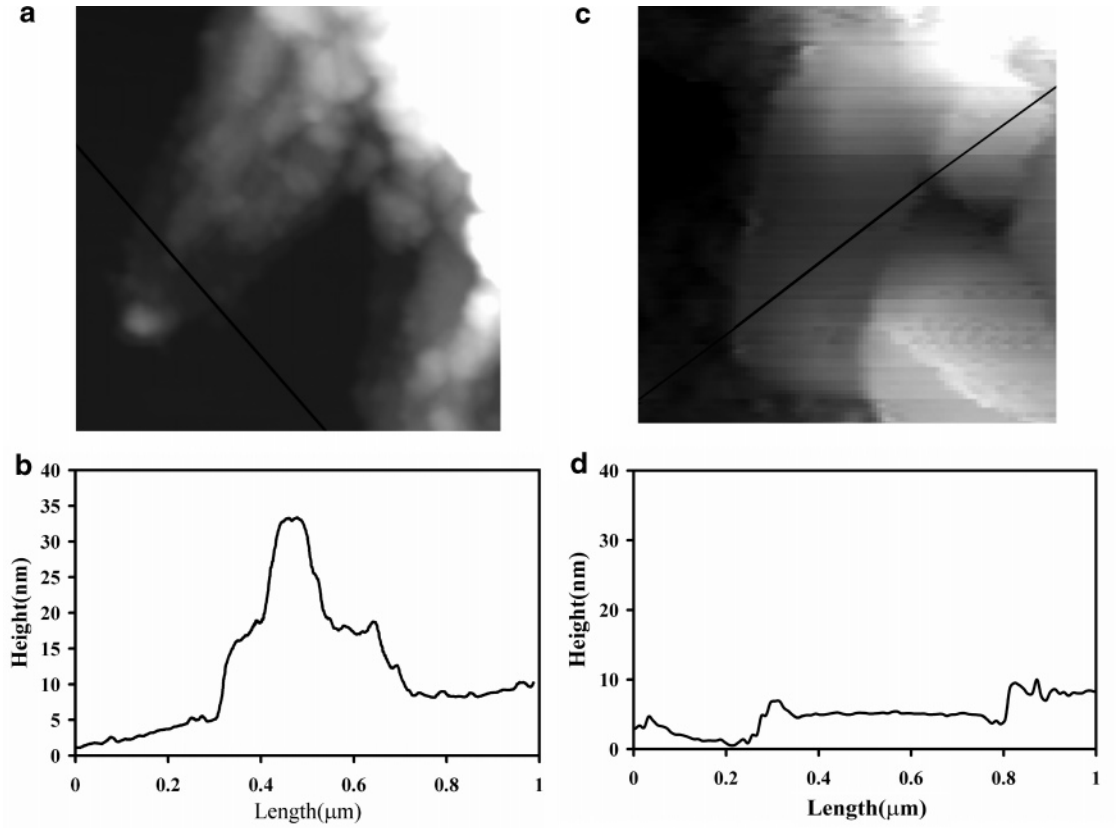

Figure 7. AFM height micrographs of crystals, along with scans of the surface height: (a) AFM height micrograph of 8AR6DA; (b) surface height scan of previous 8AR6DA image (1 μm width); (c) AFM height micrograph of 7AR10DA (1 μm width); (d) surface height scan of previous 7AR10DA image.

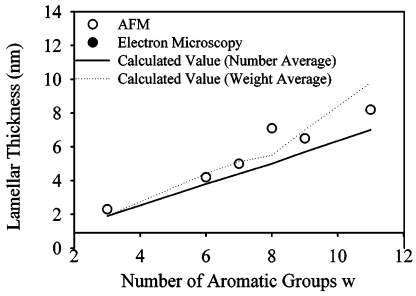

Figure 8. Changes in crystal size with block size: open cycles, AFM measurements; solid line, values calculated using repeat period of PPTA and number-average block size; dotted line, value calculated using repeat period of PPTA and weight-average block size.

the observed crystal is unilamellar. The "peak" at 7 nm may be related to tip instability, although "curling over" of the crystal edge may also be responsible, as seen in the electron microscopy image of Figure 3b. Once the tip stabilizes on the lamella surface, height remains constant around 6 nm until the tip meets a new lamella, at a length position of ~0.8 μm. The tip then rises again, eventually restabilizing on this new lamella. The important feature in this section is the stability in height throughout the crystal, in contrast with 8AR6DA and other *w*AR*n*DA, where decorations or multilamellar features were always present.

Height values of single lamellae and decorations were found to be systematically similar for a given *w* value. Average values are reported in Figure 8, where they are compared to the length of the rigid segment, as calculated using the *c* dimension of the crystal phase of PPTA, multiplied by the average number of PPTA units present in the rigid copolymer segments as determined by M_n and M_w of the rigid blocks. These were obtained using the M_n and M_w values of the macromonomers, to which a correction was applied to account for the fact that these were terephthalic acid end-capped at both ends before adding the flexible chains. A good fit is found between the AFM measurements and the values predicted using the M_w values of the macromonomers, considering experimental error, which is related to experimental methods used to evaluate the average block sizes, but also to background noise in the AFM images and to fluctuations in crystal surface regularity and positioning on the substrate. The match with M_n-derived values is not as good, experimental values being systematically higher. It must also be noted that the calculated values, depicted as dotted and full lines, are not linear, as the length of the blocks depends on the molecular weight of the macromonomers, which in turn varies with experimental conditions. The main feature here is nevertheless the regular increase in lamellar thickness with size of rigid block and the good match between observed and calculated thicknesses of the terraces or lamellae that compose the crystals, which is the most direct proof that chain folding has occurred.

Conclusion

It has been shown that, through synthetic control of the copolymer sequence, polymers with rigid segments can crystallize by chain-folding, as proven by the occurrence of lamellar thickness corresponding to the thickness of a rigid block, while the polymers contained, on average, from 2 to 3 rigid blocks.

Crystal lamellar thickness can be controlled through design of the length of the rigid sequence, but not total crystal thickness, as a tendency to in-register lamellar stacking, with crystallite overgrowths or decorations, was clearly observed. The minimum block length requirement appears to be close to one repeat unit for such rigid polymers, in contrast to more flexible chains, such

as polyethylene, where regular segments of 11 repeat units (22 methylene units) result in defective crystals, which is not the case for 22 repeat units.[12]

Finally, although polydisperse, rigid blocks crystallize readily to yield single-crystal-like structures, where were observed as being composed of many layers or lamellae. This polydispersity tolerance is tentatively attributed to both the rigidity of the crystallizable unit and its propensity to form hydrogen bonds, thus stabilizing further the nascent crystallites, whereas previous results reported in the literature show that more flexible sequences will not crystallize when polydisperse.[12]

Acknowledgment. The authors acknowledge Anne Nabet and Patricia Basque, of the CERSIM, Departement de chimie, Université Laval, for their help in X-ray and AFM characterization, of Richard Janvier, of the Pavillon Marchand, Université Laval, for assistance in electron microscopy, and of Marc D'Auteuil, of the Département de physique of Université Laval, for sample shadowing. The FFCRYST program, written by Vonk and co-workers, is also gratefully acknowledged. Funding has been provided by the Natural Sciences and Engineering Council of Canada (NSERC) and by the Fond Québécois pour la Science et la Technologie (FQRNT, formerly FCAR) of the government of Québec.

References and Notes

(1) Wilson, D.; Valluzzi, R.; Kaplan, D. *Biophys. J.* **2000**, *78*, 2690.
(2) McGrath, K. P.; Fournier, M. J.; Mason, T. L.; Tirrell, D. A. *J. Am. Chem. Soc.* **1992**, *114*, 727.
(3) Gellman, S. H. *Acc. Chem. Res.* **1998**, *31*, 173.
(4) Keller, A. *Rep. Prog. Phys.* **1968**, *31*, 623.
(5) Fischer, E. W. X. *Naturforsch.* **1957**, *12A*, 753.
(6) Keller, A. *Philos. Mag.* **1957**, *2*, 1171.
(7) Till, P. *J. Polym. Sci.* **1957**, *24*, 301.
(8) Mareau, V.; Prud'homme, R. E., In *Soft Materials: Structure and Dynamics*; Dutcher, J. R., Marangoni, A., Eds.; Marcel Dekker: New York, 2004; p 39.
(9) Ungar, G.; Xian-bing, Z. *Chem. Rev.* **2001**, *101*, 4157.
(10) Keller, A.; Foldbeck-Wood, G. In *Comprehensive Polymer Science*, 2nd Suppl.; Allen, G., Aggarwal, S. L., Russo, S., Eds.; Pergamon: Oxford, 1996; p 241.
(11) Hessel V.; Ringsdorf, H.; Festag, R.; Wendorff, J. H. *Makromol. Chem. Rapid Commun.* **1993**, *14*, 707.
(12) Le Fevere de Ten Hove, C.; Penelle, J.; Ivanov, D. A.; Jonas, A. M. *Nat. Mater.* **2004**, *3*, 33.
(13) Schmidt, R.; Decher, G.; Mésini, P. *Tetrahedron Lett.* **1997**, *40*, 1999.
(14) Lindsay, G. A.; Stenger-Smith, J. D.; Henry, R. H.; Hoover, J. M.; Nillsson, R. A.; Wynne, K. J. *Macromolecules* **1992**, *25*, 6075.
(15) Stupp, S. I.; LeBonheur, V.; Walker, K.; Li. L. S.; Huggins, K. E.; Keser, M.; Amstutz, A. *Science* **1997**, *276*, 384.
(16) Sugi, R.; Hitaka, Y.; Sekino, A.; Yokoyama, A.; Yokozawa, T. *J. Polym. Sci., Polym. Chem.* **2003**, *41*, 1341.
(17) Aharoni, S. M. *J. Polym. Sci., Polym. Phys. Ed.* **1981**, *19*, 281.
(18) Northolt, M. G.; Van Aartsen, J. J. *J. Polym. Sci., Polym. Lett. Ed.* **1973**, *11*, 333.
(19) Haraguchi, K.; Kajiyama, T.; Tayaganaki, M. *J. Appl. Polym. Sci.* **1979**, *23*, 915.
(20) Northolt, G. *Eur. Polym. J.* **1974**, *10*, 799.
(21) Hasegawa, R. K.; Chatani, Y.; Tadokoro, H. *Meet. Cryst. Soc. Jpn, Osaka, Jpn.* **1973**, 21.
(22) Liu, J.; Cheng, S. Z. D.; Geil, P. H. *Polymer* **1996**, *37*, 1413.
(23) Jackson, C. L.; Chanzy, H. D. *Polymer* **1993**, *34*, 5011.
(24) Takahashi, T.; Yamamoto, T.; Tsujimoto, I. *J. Macromol. Sci., Phys.* **1979**, *16*, 539.
(25) Tashiro, K.; Kobayashi, M.; Tadokoro, H. *Macromolecules* **1977**, *10*, 413.
(26) Boivin, J.; Brisson, J. *J. Polym. Sci., Polym. Chem Ed.* **2004**, *42*, 5098.
(27) Shashoua, V. E.; Earekson, W. M. *J. Polym. Sci., Polym. Phys. Ed.* **1971**, *9*, 2081.
(28) Cain, E. J.; Gardner, K. H.; Gabara, V.; Allen, S. R.; English, A. D. *Polym. Prepr.* **1990**, *31* (1), 518.
(29) Morgan, P. W.; Kwolek, S. L. *Macromolecules* **1975**, *8*, 104.
(30) Vonk, C. G. *J. Appl. Crystallogr.* **1973**, *6*, 148.
(31) Ruland, W. *Acta Crystallogr.* **1961**, *14*, 1180.
(32) Nakata, S.; Brisson, J. *J. Polym. Sci., Polym. Chem. Ed.* **1997**, *A35*, 2379.
(33) Nakata, S.; Brisson, J. *Polym. J.* **1997**, *29*, 663.
(34) Russo, S.; Bianchi, E.; Congiu, A.; Mariani, A.; Mendichi, R. *Macromolecules* **2000**, *33*, 4390.
(35) Chen, Y.; Baker, G. L.; Ding, Y.; Rabolt, J. F. *J. Am. Chem. Soc* **1999**, *121*, 6962.
(36) Keller, A. *Rep. Prog. Phys.* **1968**, *31*, 621.
(37) Vaughan, A. S.; Bassett, D. C. In *Comprehensive Polymer Science*; Allen, G., Bevington, J. G., Eds.; Pergamon: Oxford, 1989; Vol. 2, p 415.
(38) Bassett, D. C. In *Comprehensive Polymer Science*; Allen, G., Bevington, J. G., Eds.; Pergamon: Oxford, 1989; Vol. 1, p 841.
(39) Mareau, V. H.; Prud'homme, R. E. *Macromolecules* **2005**, *38*, 398.
(40) Sadler, D. M. *Polymer* **1983**, *24*, 1401.
(41) Frank, G. C. *J. Cryst. Growth* **1974**, *22*, 233.
(42) Waddon, A. J.; Keller, A.; Blundell, D. J. *Polymer* **1992**, *33*, 27.
(43) Jones, N. A.; Sikorski, P.; Atkins, E. D. T.; Hill, M. J. *Macromolecules* **2000**, *33*, 4146.
(44) Chum, S. P.; Knight, G. W.; Ruiz, J. M.; Phillips, P. F. *Macromolecules* **1994**, *27*, 656.
(45) Napolitano, R.; Pirozzi, B. *Macromolecules* **1998**, *31*, 3626.
(46) Koenig, J. L.; Hannon, M. *J. Macromol. Sci.* **1967**, *B1*, 118.
(47) Frayer, P.; Koenig, J. L.; Lando J. B. *J. Macromol. Sci., Phys* **1969**, *3*, 331.

MA052248K